Bulletin of Engineering Geology and the Environment (2021) 80:3293–3313
https://doi.org/10.1007/s10064-021-02140-6

ORIGINAL PAPER

A new analytical method for determination of discharge duration in tunnels subjected to groundwater inrush

Mohsen Golian[1] · Ebrahim Sharifi Teshnizi[2] · Mario Parise[3] · Josip Terzić[4] · Sasa Milanović[5] · Vesna Ristić Vakanjac[5] · Masoud Mahdad[6] · Mehdi Abbasi[2] · Hossein Taghikhani[7] · Habib Saadat[8]

Received: 30 October 2019 / Accepted: 8 February 2021 / Published online: 20 February 2021

Abstract

Unexpected water inrush to tunnels is one of the most hazardous events, especially in karst terrains that could take place during mechanized shield tunneling mostly due to inappropriate site investigations. When water inrushes to tunnel front, actions like pumping out the water or grouting, for impeding or reducing the inrush and alleviating related damages, are often time-consuming, uneconomical, difficult, or sometimes even impossible. In most cases, it is sometimes necessary to wait for lowering groundwater within the tunnel to have again the possibility to excavate. Therefore, determination of the required time for the groundwater inrush to decrease to a certain level is extremely important for tunneling management plans and plays a significant role in decision-making for project managers. In this study, an assessment of the discharge time after water inrush to tunnel using the new proposed analytical approach is argued. This method is developed based on recession analysis and hydrodynamic of open channels. For this purpose, inrush rate to tunnel front and groundwater level should be measured on at least a daily basis, a feasible and practical action to be carried out on tunnel construction sites. The method is validated with available data from three tunnels with water inrush experiences. The results show that the analytically determined water inrush regime is in good accordance with the observed ones.

Keywords Tunneling, · Water inrush, · Groundwater level, · Recession analysis, · Exponential equation

Introduction

Water inrush is a sudden and often overwhelming flow of water into underground workings (the Mindat Glossary). Water inrush (usually with mud gushing) is one of the geological disasters that can be faced in underground engineering works which might impose huge impacts on construction timetable, financial plan, and on project safety as well (Hou et al. 2016). This event is particularly emphasized in karst terrains where, because of high heterogeneity and anisotropy of karstified rock masses (Bakalowicz 2005; Ford and Williams 2007), the occurrence of unexpected events is prevalent (Parise et al. 2015a). Serious water inrushes during the tunnel construction can result in human casualties and financial losses (Hou et al. 2016). Table 1 represents a history of water inrush events in some tunnels with causes, casualties, and consequences.

Therefore, the resumption of excavation depends on the relative discharge of water inrush to the tunnel face. Because in tunneling projects, downtime of the tunnel boring machine (TBM) causes high financial loss, knowing the discharge time

✉ Mohsen Golian
mohsen.golian@gmail.com

[1] Tehran Science and Research Branch, Islamic Azad University, Tehran, Iran

[2] Department of Geology, Faculty of Science, Ferdowsi University, Mashhad, Iran

[3] Department of Earth and Environmental Sciences, University Aldo Moro, Bari, Italy

[4] Croatian Geological Survey, Sachsova 2, HR-10000 Zagreb, Croatia

[5] Department of Hydrogeology, Faculty of Mining and Geology, Centre for Karst Hydrogeology, University of Belgrade, Djušina 7, Belgrade 11000, Serbia

[6] Iran University of Science and Technology, Tehran, Iran

[7] Department of Geology, Tarbiat Modares University, Tehran, Iran

[8] Shiraz University, Shiraz, Iran

Table 1 Documented water inrush events in some tunnels with their causes and consequences

Tunnel[a]	Country	Causes, casualties, and consequences	Reference
Gibei	Romania	Compact fissured clay layer failed suddenly, allowing water inrush more than 0.01 m^3/s into the tunnel, 6 months delay in the project schedule	Clay and Takacs (1997)
Motorway	Austria	650 m^3 of loose material collapsed, resulting in water inrush of up to 0.025 m^3/s, project schedule delays	
Orange fish	South Africa	Heavy water inrush of about 0.92 m^3/s into the tunnel at 14 bars pressure, Entire 1.6 km tunnel section flooded within 24 hours	
Dayaoshan	China	Water inrush induced by excavating in a water-rich zone completely submerged the vertical	Xu and Huang (1996)
Yichang–Wanzhou		Two extraordinarily serious disasters happened during the tunnel construction, resulting in 21 deaths	Qiang and Rong (2008)
Yuan-Liang-Shan		71 water inrush events, 9 men died, maximum water pressure 4.6 MPa, maximum water emission 0.83 m^3/s	Li et al. (2016); Shi et al. (2017)
Wu-Long		10 water inrush events, maximum water inrush of 83.1 m^3/s, economic loss of 20 million RMB	
Ma-Lu-Jing		19 water inrush events, 15 men died, 2 years of delay in the project	
Da-Zhi-Ping		14 water inrush events, maximum water inrush of 4.2 m^3/s, mud emission of 14000 m^3	
Daba		Heavy rain triggered some potential water outlets, causing a serious water inrush, the total quantity of inrush sharply increased to 4.17 m^3/s	Li et al. (2018)
Chaoyang		Heavy flood of water and mud, damage to equipment, three casualties	Zhang et al. (2020)
Milwaukee	USA	Average water inrush reached 0.051 m^3/s in the North Shore tunnel, halting the construction for four months	Day (2004)
Hsuehshan	Taiwan	TBM seriously damaged due to tunnel collapse and groundwater inrush of 0.75 m^3/s to the tunnel, 11 men died	Taneeb (2005)
Moncalvo	Italy	Water and mud inrush of approximately 60,000 m^3 invaded an underground gypsum quarry. A large sinkhole (20 m wide and 10 m deep) formed at the surface	Bonetto et al. (2008); Vigna et al. (2010a, b)

[a] All of these events associated with the karst geo-hazard

after the water inrush is of high importance. Water discharge time estimation will help project managers to instantly make appropriate decisions and be able to maintain the excavation process as scheduled or, at least, mitigate the delays.

The occurrence of water inrush during tunnel excavation could be prevented where there is accurate and detailed knowledge on the local geology, from both the hydrogeological and engineering geological point of view. However, in complex geological settings, there might always be a certain amount of unpredictability, due to insufficient data, spatial and temporal variability of hydrogeological properties, complexity in the groundwater flow paths, the position of main conduits, and speleogenesis (Milanović and Vasić 2016; Milanović 2016), or due to a combination of the above, especially in karst terrains. Based on the statistics data, up to the end of 2008 in China, nearly half of tunnels in construction and operation had encountered large-scale water inrushes

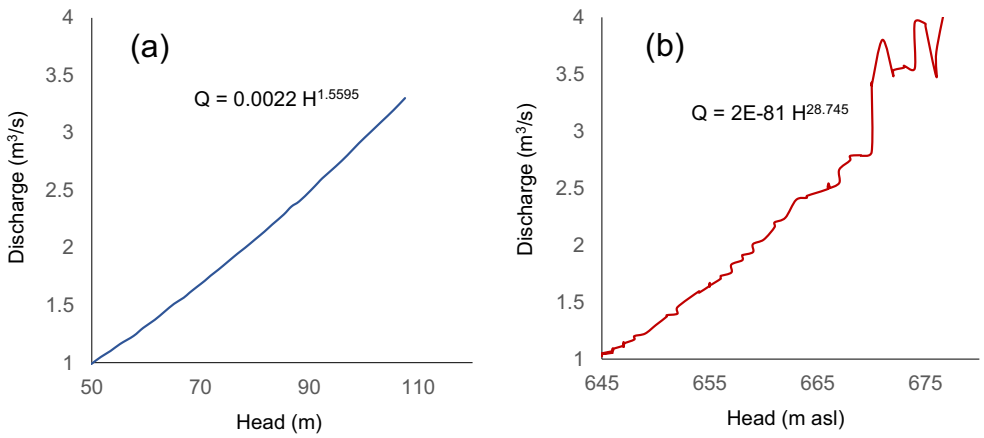

Fig. 1 Head-discharge relationship for **a** a 1.2-m Parshall Flume device and **b** the Nosud Tunnel

in karst areas, because of complexities in these natural setting, and difficulty in reaching a full understanding of the hydrogeological properties (Li et al. 2016).

Water inrush in tunnels can be particularly difficult to manage in the karstified rock mass and weakened fault zones, rich in groundwater and with high permeability (Zhao et al. 2013; Li et al. 2016; Wang et al. 2017). In detail, karst environments are highly prone to these situations, due to the great heterogeneity of karst aquifers, and unpredictability of the groundwater paths in karst aquifers, even with the possibility to reactivate the previously dry passages and conduits, in consequence of the hydrogeological changes caused by the tunnel construction (Waltham and Smart 1988; Milanović 2000, 2002; De Waele et al. 2011; Parise et al. 2015a, b, 2018). In addition to imposing delays in the construction of engineering works, related damages, and casualties, these events might also progressively move upward, eventually producing consequences at the ground, and originating sinkholes (Wang et al. 2008; Vigna et al. 2010a; Gutierrez et al. 2014; Parise 2019).

Similar to the flow rate recession of karst springs (Fiorillo 2014; Stevanović 2015), there is a sudden drop in inrush rate in a short period, which is due to draining of that part of the aquifer in the immediate surroundings of the tunnel. Over time, water inrush to the tunnel decreases slowly and reaches a constant rate, when the impacted aquifer reaches a new condition of equilibrium with the tunnel. Due to the need for a proper method that can be used to estimate the groundwater discharge time after the inrush, a new method considering the nature of the recession curve is introduced in this study.

Methodology

Hydrodynamic of conduit flow

Water inrush in tunnels is often due to an encounter of the tunnel face with a karst conduit or conduit fault (McCallum et al. 2016; Milanović 2016). In conduit flow systems, where

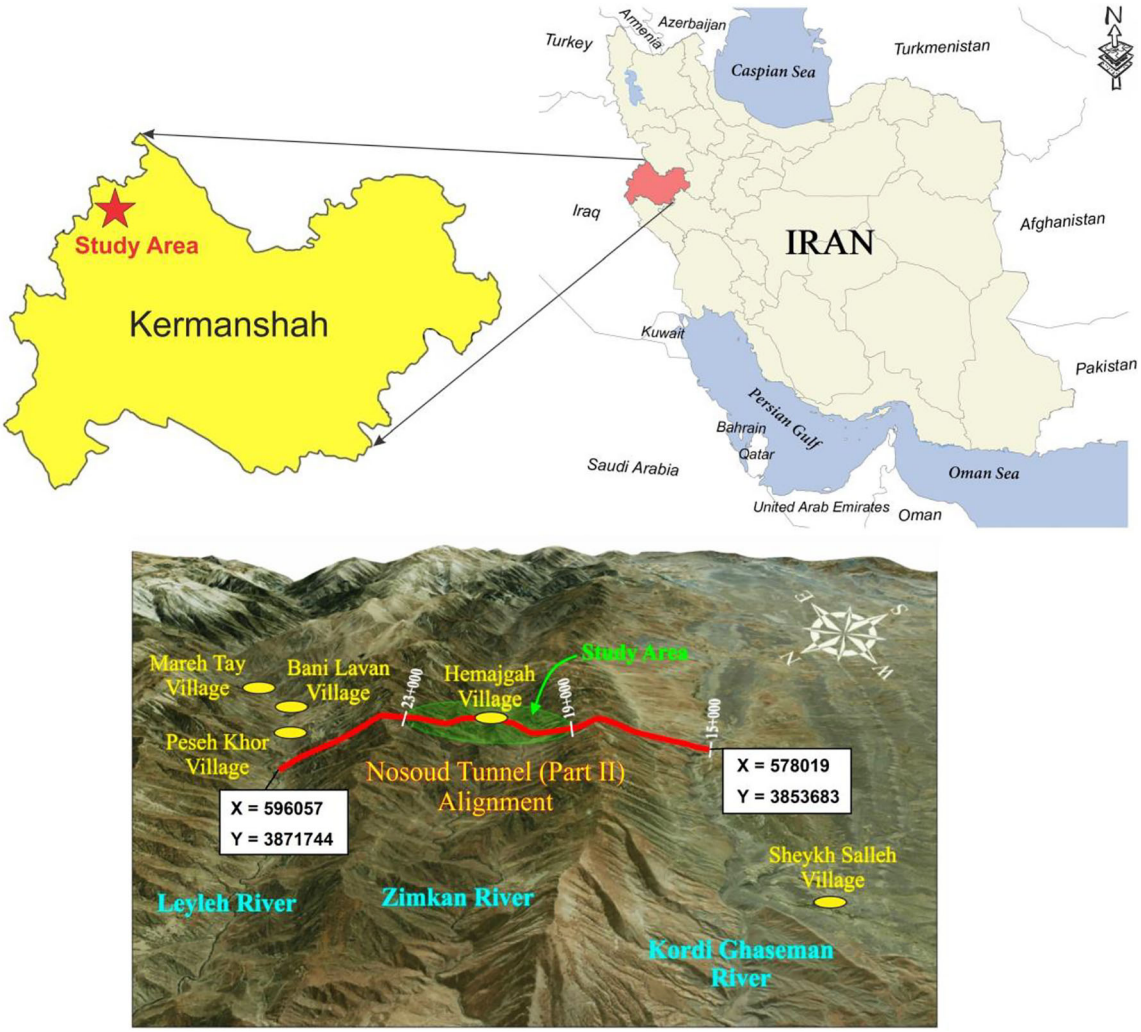

Fig. 2 Location map and satellite image of the second stretch of the Nosud tunnel

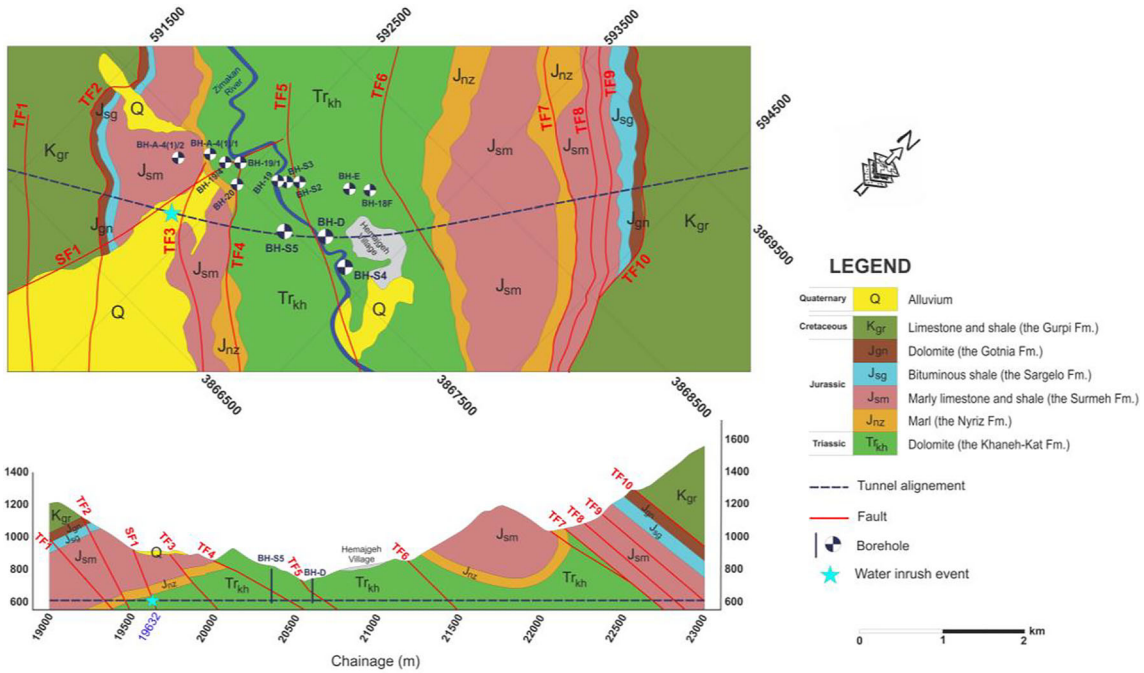

Fig. 3 Geological map and profile of the Nosud Tunnel in the Zimakan Valley (chainage 19 to 23 km)

predominantly turbulent flow conditions prevail, especially at the local, applying Darcy's law (and equations developed on it) is not correct due to the high proportion of turbulent flow, which contradicts the limitations of the laminar flow assumptions (Fanchi 2002; Giese et al. 2018). Conduit flow especially prevails in the first minutes or hours of the inrush, but due to emergency, usually, no monitoring is possible at that moment. After that first period, a higher proportion of groundwater inrush generates from the rock mass (consisting of numerous mutually connected discontinuities and karstic voids), and the inrush becomes more predictable; in some approximate way, the flow can be subjected to mathematical approach study. The scale issue becomes more and more important (Sauter 1992; White 2002), also due to the difficulty in identification of the hydrologic catchment boundaries in karst. Results of investigations showed that the hydrodynamics of flow in conduit-flow prevailing media can be described or simulated based on the hydrodynamics of pipes or in open channels. For instance, McCormack et al. (2017) developed a two conduit network model based on the hydrodynamics of open channels that simulated the main karst conduit flow system and discharge from a conduit fault in the Bell Harbour watershed in western Ireland, using a complex network of pipes (representing karst conduits), drainage channels (representing faults) and tanks (representing lakes). Also, 3D and mathematical modeling of karst conduit spatial position, as well as model of flows, was obtained and serve as a foundation for the simulation of technological processes in defining groundwater seepage pathways in the Višegrad dam rehabilitation process (Milanović and Vasić 2016). Besides, Perriquet (2014), using recession analysis, observed conduit hydrodynamic behavior in some boreholes drilled in the Bell Harbour

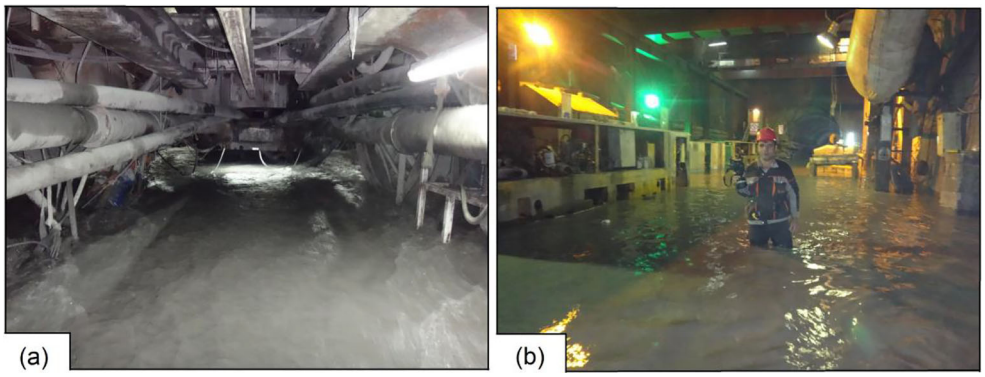

Fig. 4 Water inrush to **a** TBM Back up utilities and **b** the tunnel cavern area

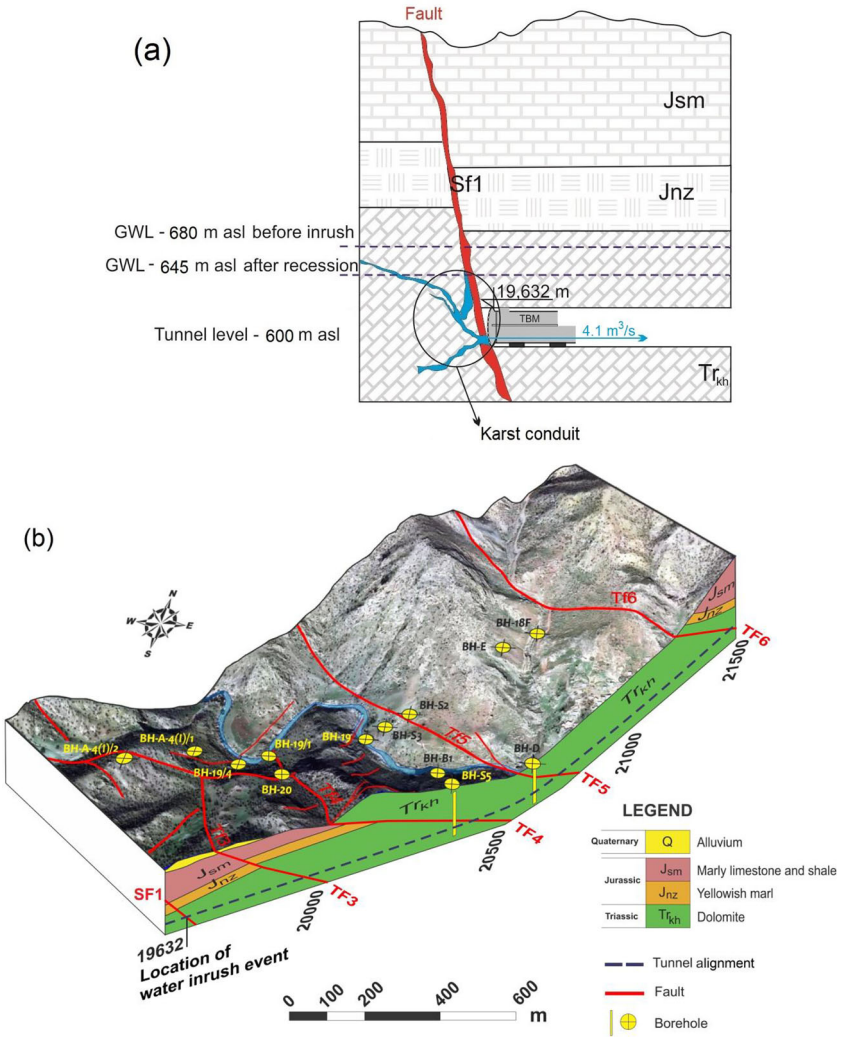

Fig. 5 **a** Schematic proposal and **b** 3-D block diagram of the Zimakan Valley, showing the tunnel route and stopping location of the inrush site in the Zimakan Valley

watershed. On the other hand, it is generally accepted that the flow under pressure karst conduits can be simulated by the Darcy-Weisbach equation (Harmon and Wicks 2006).

Determining water inrush discharge time during the tunnel construction

By experience, it can be stated that the drawdown of tunnel inrush water level is exponential within in time (Li et al. 2018). Recession curve analyses are common in karst hydrogeology, especially exercised for estimation of karst spring regime. There are several equations, used for over a century (Boussinesq 1904; Maillet 1905; Mangin 1975; Dewandel et al. 2003). Still, using them as they are for the water inrush calculations during the tunnel construction works does not seem plausible, because the monitoring time is too short and does not comprise all the components of the recession curve, and especially not the master regression curve. Nevertheless, the relation of the inrush recession in a tunnel over time, similarly to the discharge recession relation of a karst spring (Maillet 1905), can be described by an exponential equation as follows:

$$Q(t) = Q_0 e^{-\alpha t} \quad (1)$$

where $Q(t)$ and Q_0 are the inrush rate [L^3T^{-1}] at time t and the initial inrush rate at an earlier time, respectively and α is the recession coefficient [T^{-1}].

Using this equation, it is possible to assess the time required for reaching the inrush to a level that makes possible recovery of the tunnel operation. The equation can be achieved by the following steps after a short period of daily groundwater level (GWL) monitoring in boreholes and water inrush rate into the tunnel.

Step 1: Determining the relation of groundwater level drawdown in time

During the recession of water inrush, the GWL hydrograph component in nearby boreholes had a recession that can be

Fig. 6 A view of the karst conduit causing the water inrush to the tunnel at chainage 19.632 km

approximated by a simple exponential equation as below (Degallier 1966):

$$H = H_0 e^{-\propto t} \quad (2)$$

where H_0 and H are the measured GWL [L] in the borehole at the beginning of the measurement period and after a certain time (t), respectively. The linear form of the above equation can be determined as follows:

$$\ln(H) = \ln\left(H_0 e^{-\propto t}\right) \rightarrow \ln(H) = -\propto t + \ln(H_0) \rightarrow \ln(H) = -\propto t + D \quad (3)$$

where D is a constant equal to $ln(H_0)$ To obtain this equation, one should draw a natural logarithm of the observed GWL against time in a graph and determine its linear regression.

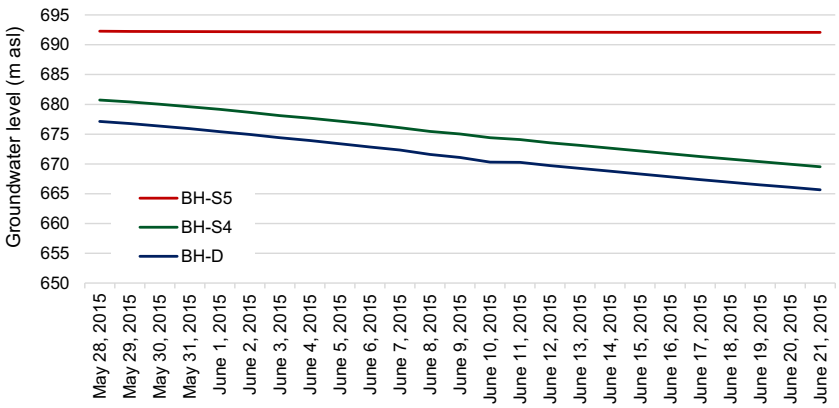

Fig. 7 GWL recession in the BH-S5, BH-S4, and BH-D boreholes from May 28 to June 21, 2015

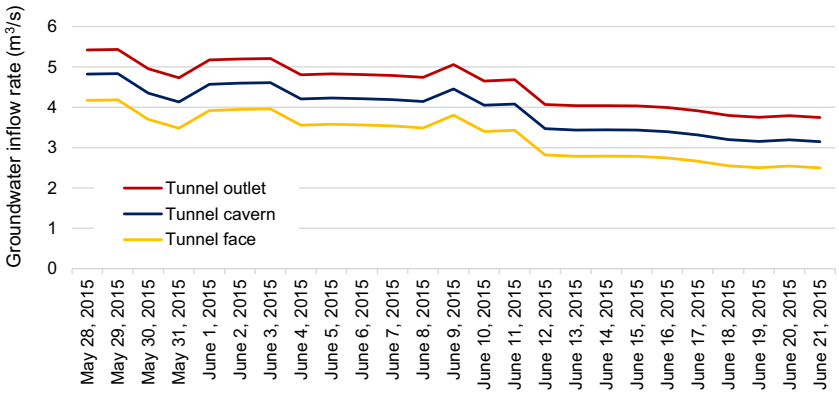

Fig. 8 Inrush rate measured at different locations in the tunnel from May 28 to June 21, 2015

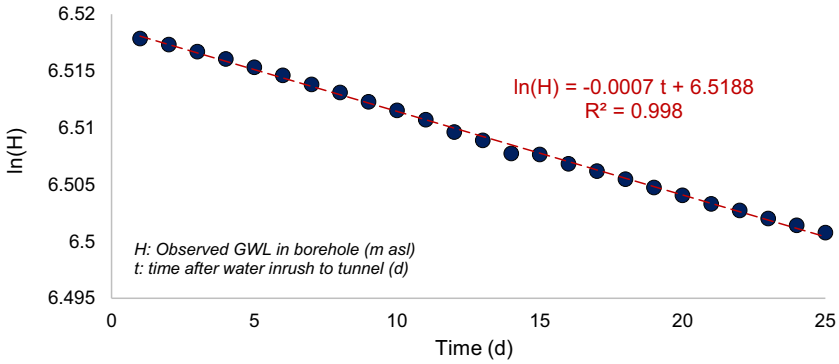

Fig. 9 Correlation diagram of the natural logarithm of GWL in the BH-D borehole versus time

Step 2: Determining the relation of water inrush recession and groundwater level drawdown

Since conduit flow hydrodynamics in karstic conduits and conduit faults can be modeled in a way similar to the hydrodynamics of pipes or open channels, after extensive evaluations the developed simple power equation for Parshall Flume (Parshall 1928) and the Darcy-Weisbach equation was used to express the relationship of the inrush rate to the tunnel and its corresponding hydraulic head measured in adjacent boreholes (Fig. 1):

$$Q = CH^{n} \tag{4}$$

$$r\,Q^{2} = H \tag{5}$$

$$r = {}^{8fL}\!/_{D^{5}\pi^{2}g} \tag{5a}$$

where C is the free-flow coefficient for Parshall Flume, n is Parshall Flume power constant, f is Darcy–Weisbach friction factor, L is pipe length [L], D is hydraulic diameter [L], and g is the gravitational acceleration [LT^{-2}]. If inrush is fully turbulent, r can be considered a constant. The linear form of the above equations can be determined as follows:

$$\ln(Q) = \ln\left(CH^{n}\right) \rightarrow \ln(Q) = n\ln(H) + \ln(C) \rightarrow \ln(Q) = n\ln(H) + E \tag{6}$$

$$\ln\left(r\,Q^{2}\right) = \ln(H) \rightarrow 2\ln(Q) + \ln(r) = \ln(H) \rightarrow \ln(Q) = 0.5\ln(H) + A \tag{7}$$

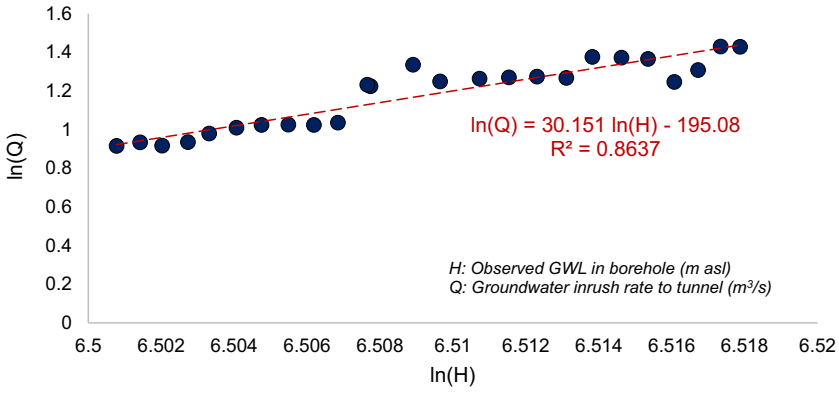

Fig. 10 Correlation diagram of the natural logarithm of GWL in BH-D borehole and the natural logarithm of inrush rate to the tunnel face

Table 2 Calculated inrush rate to the Nosud tunnel face over time

Days after water inrush[a]	Inrush rate (m^3/s)		Days after water inrush	Inrush rate (m^3/s)	
	Cal.	Obs.		Cal.	Obs.
1	4.249	4.170	50	1.511	1.641
10	3.514	3.560	60	1.224	1.201
20	2.846	2.745	70	0.991	1.081
30	2.118	2.200	80	0.802	1.054
40	1.866	1.760			

[a] The first day was May 28, 2015

where *E and A* are constants equal to *ln (C)* and *-0.5 ln (r)*, respectively. As seen, Eqs. 6 and 7 are similar; however, the logarithmic form of the Parshall Flume equation is the general form, which is considered in this study. Therefore, one should draw a natural logarithm of the observed inrush rates and a natural logarithm of the observed GWL in the graph, and determine its linear regression equation.

Step 3: Determining the relation of water inrush recession in time

By integrating Eqs. 3 and 6, the exponential equation of the water recession can be determined.

$$\ln(Q) = n(-\propto t + D) + E \rightarrow \ln(Q) = -(\propto n)t + (nD + E) \rightarrow \ln(Q) = -Ft + G \rightarrow Q = e^{-Ft+G} \rightarrow Q = e^{G} \times e^{-Ft} \rightarrow Q = Ie^{-Ft} \quad (8)$$

where F, G, and I are constants equal, respectively, to αn, $nD+E$, and e^G.

For a clearer understanding, the method of determining water discharge time is described in the three following case studies.

Case studies

The described method was first developed for the Nosud tunnel (Iran) and later for further validation applied to the Headrace tunnel (Sri Lanka) and the Glas tunnel (Iran).

Case study 1: The Nosud Tunnel

The Nosud project is one of the most important water supply projects in Iran, located in the northwest of Kermanshah province, near the Iran-Iraq border. According to the plan, it is expected to transfer the Sirwan River water after having it stored at the Daryan Dam, using the Nosud gravity water conveyance tunnel for a length greater than 49 km, with a slope of about 0.082%. The tunnel consists of three parts. Excavation of the second stretch of the tunnel is approximately 25.7 km long, with a boring diameter of 6.73 m and a final diameter of 6 m. The Zimakan Valley study area is located approximately at the chainage 19 to 23 km, of the second stretch of the tunnel, as shown in Fig. 2.

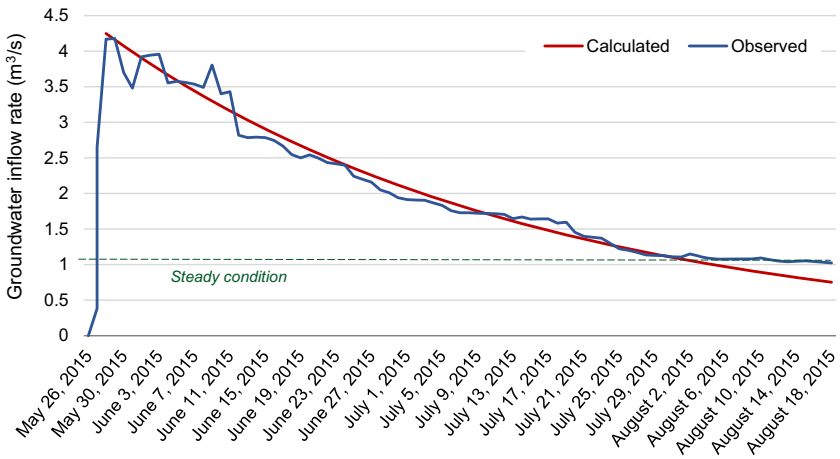

Fig. 11 Calculated versus observed water inrush rate over time (from May 26 to August 18, 2015)

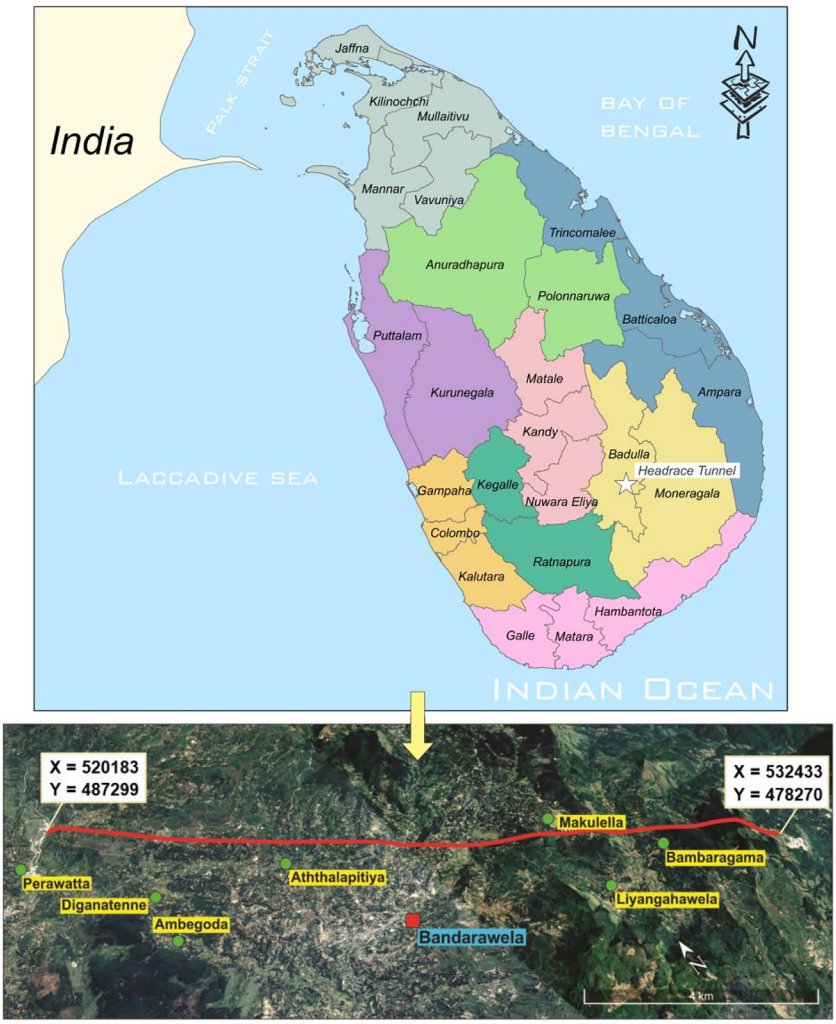

Fig. 12 Geographical location and satellite image of the HRT

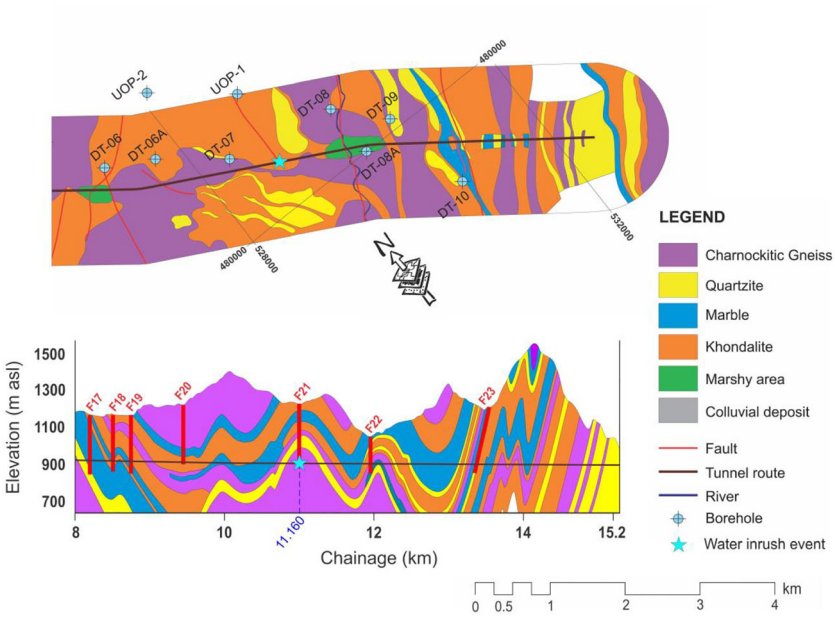

Fig. 13 Geological map and profile of the HRT

Fig. 14 Water inrush to the outlet TBM face at chainage 11.160 km of the tunnel

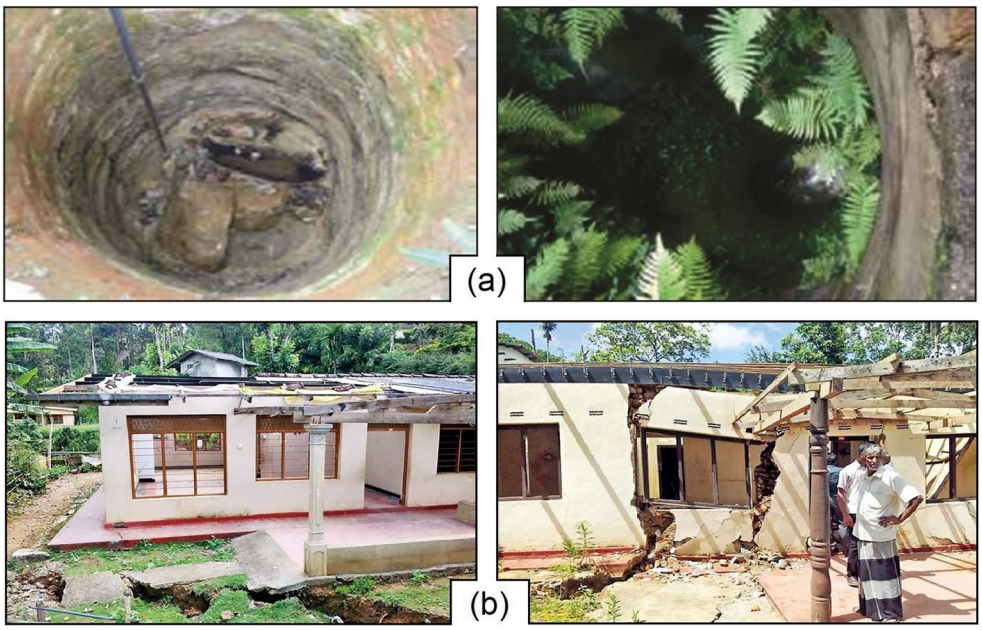

Fig. 15 Some environmental and geotechnical consequences of the HRT excavation; **a** drying up of domestic wells near the tunnel route (Rathnayake 2016), and **b** ground subsidence and damage to residential buildings (Ismail 2017)

Geological characteristics of the study area

The rock outcrops along the tunnel way in the Zimakan Valley include the Surmeh (J_{sm}), the Nairiz (J_{nz}), and the Khan-e-Kat (Tr_{kh}) Formations. (Fig. 3). The Surmeh Formation consists of marly limestone and shale with an overall thickness of about 400 m. Below this unit, marls of the Nairiz Formation are presented with an overall thickness of about 50 m (Sadeghi et al. 2020). The oldest lithotypes in the area are the Triassic dolomites belonging to the Khan-e-Kat Formation. In the Zimakan Valley, most of the tunneling problems have occurred in the Khan-e-Kat Formation, affected by faulting and karst.

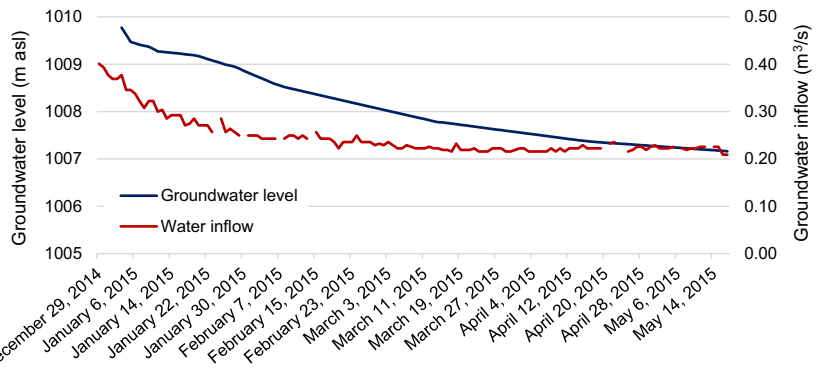

Fig. 16 Hydrographs of measured GWL in DT-08 borehole and observed water inrush rate to the tunnel face

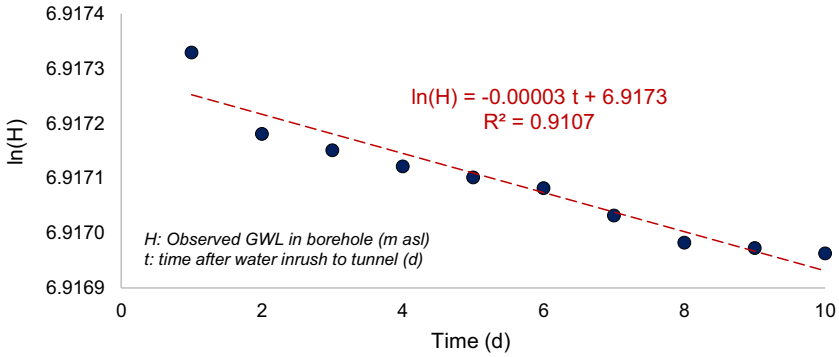

Fig. 17 Correlation diagram of the natural logarithm of GWL in DT-08 borehole versus time

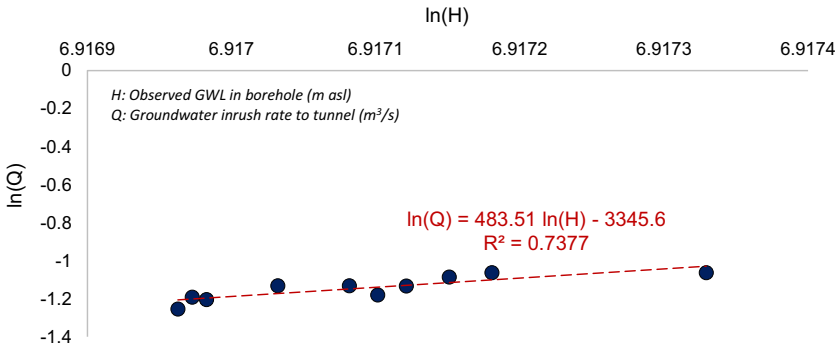

Fig. 18 Correlation diagram of the natural logarithm of GWL in the DT-08 borehole and natural logarithm of inrush rate to the tunnel face

Event of groundwater inrush into the tunnel

In late May 2015, excavation operation of the Nosud tunnel at chainage 19.632 km in the Zimakan Valley stopped due to the sudden water inrush of about 4.1 m^3/s to the TBM face leading to serious damages to construction equipment and machinery and imposing a serious delay of about four months to the project (Fig. 4). At this point, TBM encountered a karst conduit in the Khan-e-Kat formation (Figs. 5 and 6). In crisis management meetings held after the event, all emergency plans and decisions depended upon the time needed for water inrush discharge; therefore, estimation of the time became a priority for the committee.

Determining the water inrush discharge time

According to GWL monitoring in boreholes along the tunnel route in Zimakan Valley (Fig. 7), the BH-S4 and BH-D boreholes had a similar GWL decrease rate which was different from the BH-S5 borehole (location of boreholes is presented

Table 3 Calculated inrush rate to the Headrace tunnel face over time

Days after water inrush[a]	Inrush rate (m^3/s)		Days after water inrush	Inrush rate (m^3/s)	
	Cal.	Obs.		Cal.	Obs.
1	0.357	0.333	45	0.189	0.243
5	0.337	0.317	50	0.175	0.236
10	0.313	0.304	55	0.163	0.236
15	0.291	0.292	60	0.152	0.236
20	0.271	0.271	65	0.141	0.226
25	0.252	0.264	70	0.131	0.222
30	0.234	0.250	75	0.122	0.232
35	0.218	0.243	80	0.113	0.216
40	0.203	0.243	45	0.106	0.243

[a] The first day was January 3, 2015

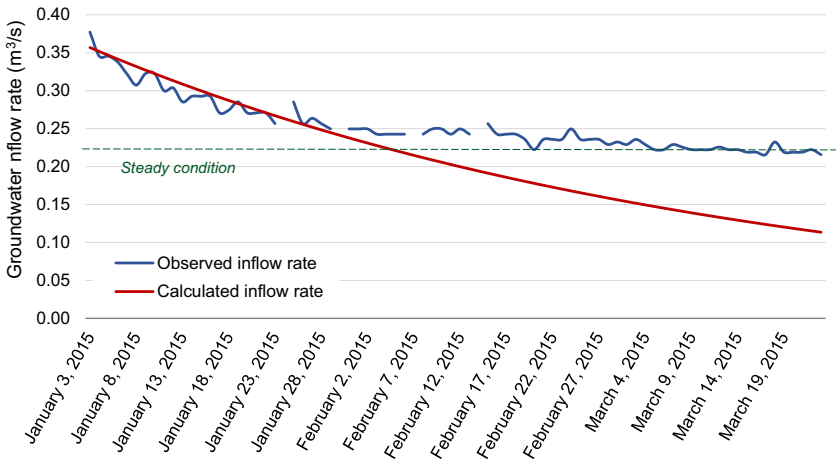

Fig. 19 Comparison diagram of observed water inrush rate to the tunnel face over time versus calculated ones

in Fig. 5). Figure 7 shows hydrographs of GWL in BH-S5, BH-D, and BH-S4 boreholes. According to the BH-S4 and BH-D level changes, a GWL loss of 11.5 m occurred from May 28 to June 21, 2015, over 25 days. The GWL decrease in the BH-S5 borehole, on the other hand, was about 0.2 m. The reason for this difference was unknown, but it can assume that BH-S5 is out of the main karst preferential flow paths. It is also notable that the GWL decrease was close to linear, pointing to the fact that the outflow was mostly dictated by the hydraulic resistance of the karst features and the hosting rock mass. Figure 8 shows the hydrograph of the measured inrush rate at different locations in the tunnel. An amount of 7.1 million m^3 of water, almost equal to the water consumption of Tehran metropolitan in three days, discharged from the tunnel in these 25 days. Water inrush measurement was carried out using the water current meter.

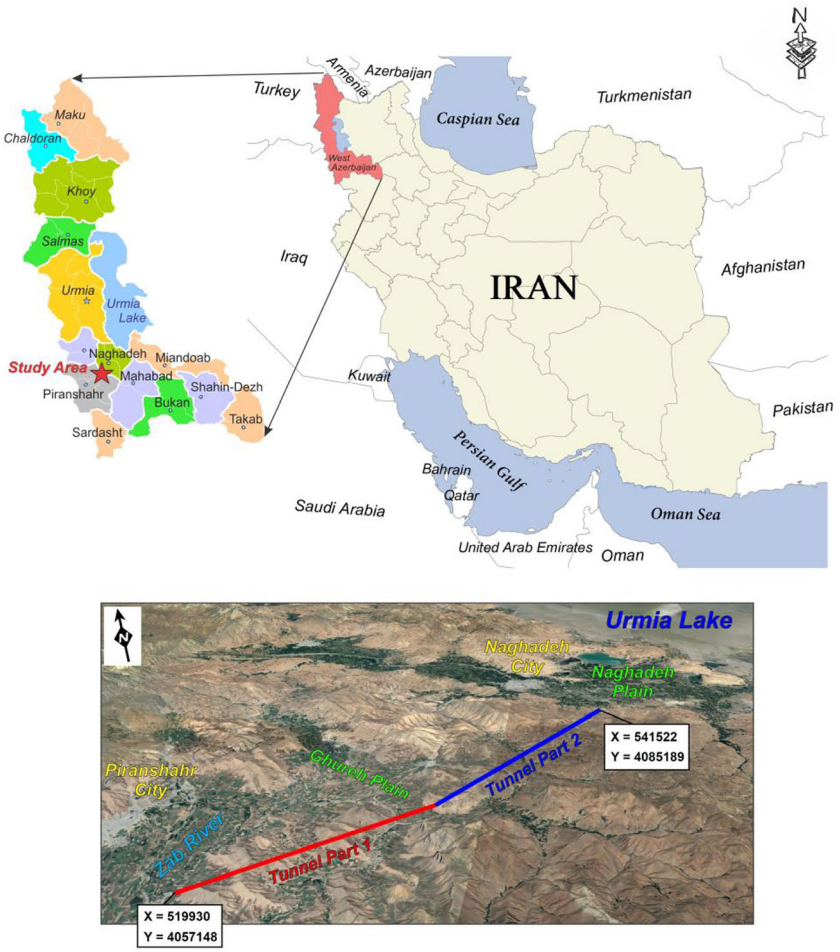

Fig. 20 Geographical location and satellite image of the Glas tunnel

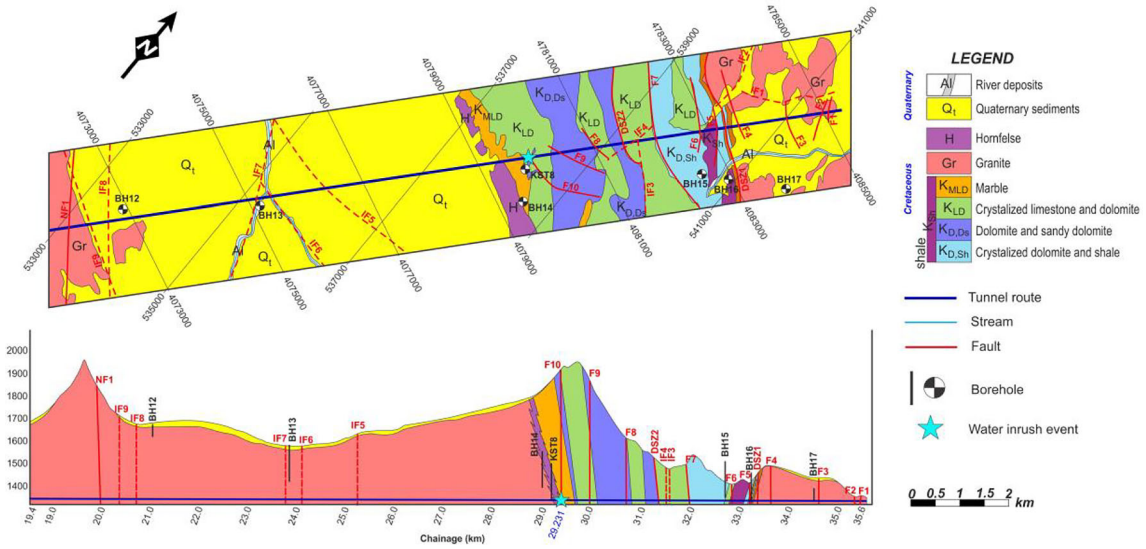

Fig. 21 Geological map and profile of the outlet stretch of the Glas tunnel

Twenty-seven days after the inrush event, based on daily monitoring data, the required time for tunnel inrush recession in the tunnel was calculated, using the method here presented. Therefore, the linear equation of the natural logarithm of GWL against time was derived for the BH-D borehole (Eq. 9; Fig. 9). Then, changes in the natural logarithm of the inrush rates were fit to the changes in the natural logarithm of GWL (measured in the BH-D), and the linear equation correlating these parameters was determined (Eq. 10; Fig. 10). Finally, the exponential recession equation of water inrush against time was derived by substituting two equations, and through related simplification (Eq. 11).

Step 1: determining the linear form of simple exponential equation of observed groundwater level drawdown in time (refer to Eq. 3):

$$\ln(H) = -0.0007\,t + 6.5188 \tag{9}$$

Step 2: determining the linear form of simple power equation between observed water inrush and observed groundwater level drawdown (refer to Eq. 6):

$$\ln(Q) = 30.151\,\ln(H) - 195.08 \tag{10}$$

Step 3: determining the simple exponential equation of water inrush recession in time by substituting two above equations (refer to Eq. 8):

Fig. 22 A view of the karst conduit causing the water inrush to the tunnel at chainage 29.231 km

Fig. 23 Water inrush to **a** TBM Back up utilities, and **b** the tunnel outlet

$$\ln(Q) = 30.151\ (-0.0007\ t + 6.5188) - 195.08 \rightarrow \ln(Q) = -0.0211\ t + 1.47 \rightarrow Q = 4.34e^{-0.0211\ t} \quad (11)$$

The noble design of water drainage equipment in double shield TBM of Nosud tunnel made it possible to pump out the water at a maximum rate of 0.8 m^3/s. Therefore, the required time to decrease the inrush rate to 0.8 m^3/s was calculated using the exponential equation in at least 80 days, as shown in Table 2 (equal to August 18, 2015). In Fig. 11, the calculated rescission of water inrush from May 28 to August 18, 2005, was compared with the observed one. It can be noted that from August 11, 2015, the inrush rate reached a constant value of about 1 m^3/s.

Following the tunnel excavation process, TBM encountered several caves and karst conduits, which were dry or with a small amount of water.

Case study 2: The Headrace Tunnel

The Headrace tunnel (HRT), with a length of about 15.4 km, is located in the southern part of Badulla administrative district in the province of Uva, Sri-Lanka (Fig. 12). HRT is part of the hydro-mechanical Uma Oya Multipurpose Development Project (UOMDP), operating as a pressure tunnel to convey water from the Dyraaba dam to a pressure shaft followed by a 120MW underground powerhouse. This project aims to improve the irrigation of 20.2 km^2 of agricultural land, transfer 145 million m^3 water, and generate 290 GW/h of power in a year (Golian et al. 2021b). Excavation of HRT was finished by two Double Shield TBMs (called M1684 and M1685) with an excavation diameter of 4.3 m from two sides (inlet and outlet). The main hazards concerning HRT were unpredictable geological conditions and the possibility of water inrush.

Geological characteristics of the study area

The HRT is located in the Highland Complex (HC) lithological unit of central Sri-Lanka, characterized by the presence of gneisses, ranging from charnockitic gneiss to quartzofeldspathic gneiss and garnet-sillimanite-biotite-graphite gneiss (the Khondalite unit), with some parts containing undifferentiated gneiss. Generally, these rocks are locally interlayered with marble and quartzite. From the structural-geological standpoint, the study area shows a poly-phase ductile deformation history,

Fig. 24 Ground subsidence near the tunnel route due to the water inrush

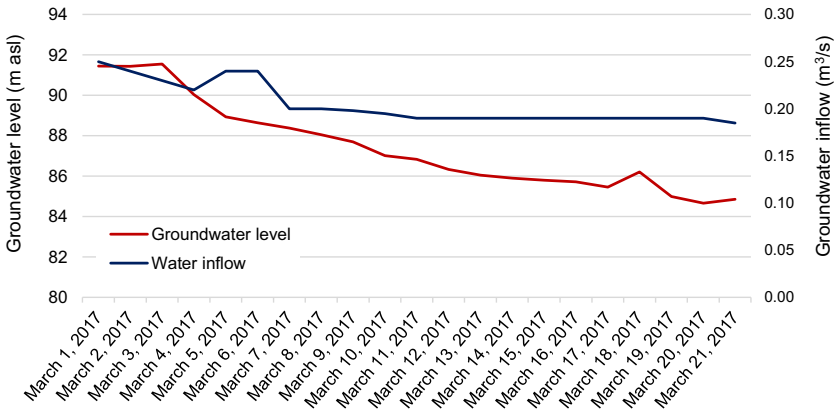

Fig. 25 Hydrographs of measured GWL in KST-08 borehole and observed water inrush rate to the tunnel face

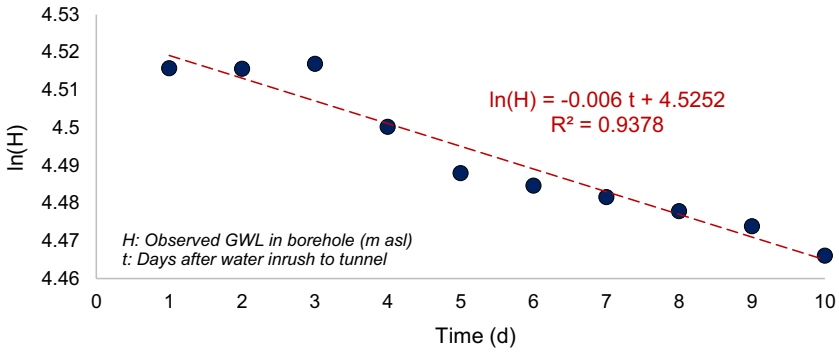

Fig. 26 Correlation diagram of the natural logarithm of GWL in the KST-08 borehole versus time

characterized by large scale folding and thrusting. Rock bands of the area display their main foliation (S) which could be related to the main deformation phase. The geological map and profile of the tunnel from chainage 8 km to the outlet are shown in Fig. 13.

Event of groundwater inrush to the tunnel

On December 24, 2014, a water inrush of about 0.4 m^3/s occurred at a chainage of 11.160 km (Fig. 14). This event caused serious delays in the excavation process. At the site, TBM encountered a high permeable fault zone in gneiss. After 80 days, the measured water outflow by Parshall Flume at the tunnel outlet reduced to about 0.216 m^3/s. Subsequently, GWL in DT-08 borehole decreased to approximately 2 m. GWL drawdowns due to the tunnel excavation caused ground subsidence, and domestic water wells drying up near the tunnel route (Golian et al. 2021b; Fig. 15).

Recession time estimation of the water inrush

When water inrush occurred in the tunnel, changes in its rate and the GWL drawdown in DT-08 borehole were monitored daily (Fig. 16). Using the gathered data from January 3 to 12, 2015 (10 days), the presented method was applied with the calculations presented in Eqs. 12 to 14, while the hydrographs, and diagrams, and the various comparisons are shown in Figs. 17 and 18.

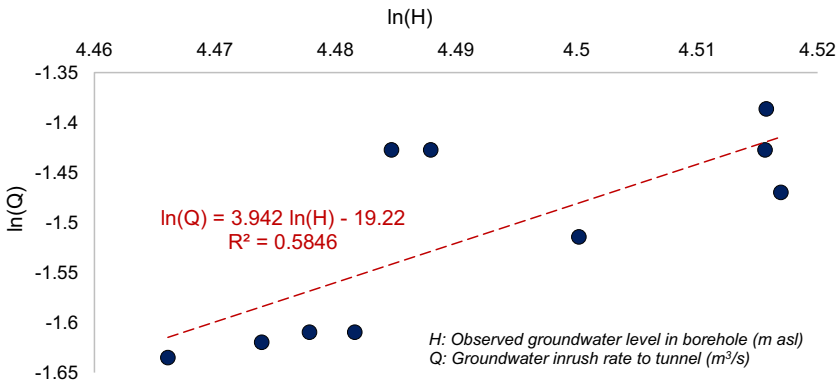

Fig. 27 Correlation diagram of the natural logarithm of GWL in the KST-08 borehole and the natural logarithm of water inrush rate to the tunnel face

Table 4 Calculated inrush rate to the Glas tunnel face over time

Days after water inrush[a]	Inrush rate (m^3/s)		Days after water inrush	Inrush rate (m^3/s)	
	Cal.	Obs.		Cal.	Obs.
1	0.245	0.250	13	0.184	0.190
3	0.234	0.230	15	0.176	0.190
5	0.223	0.240	17	0.168	0.190
7	0.213	0.200	19	0.160	0.190
9	0.203	0.198	21	0.153	0.185
11	0.193	0.190			

[a] The first day was March 1, 2017

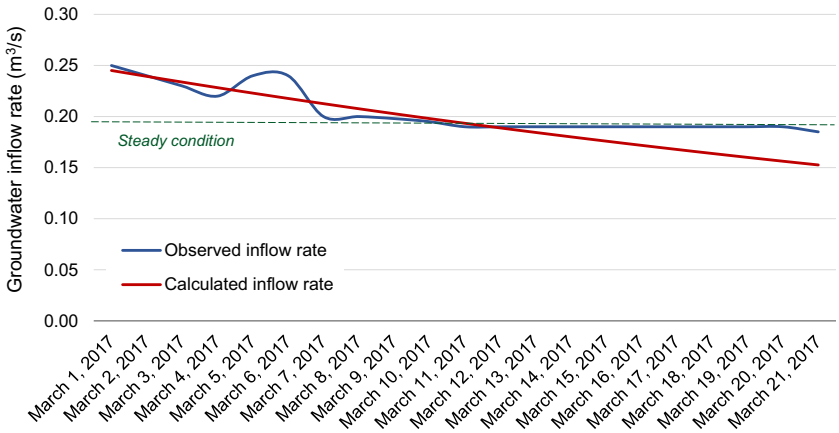

Fig. 28 Comparison diagram of observed water inrush rate to the tunnel face over time versus calculated ones

$$\ln(H) = -0.00003\,t + 6.9173 \quad (12)$$

$$\ln(Q) = 483.51\,\ln(H) - 3345.6 \quad (13)$$

$$\ln(Q) = 483.51\,(-0.00003\,t + 6.9173) - 3345.6 \rightarrow \ln(Q) = -0.0145\,t - 1.02 \rightarrow Q = 0.36\,e^{-0.0145\,t} \quad (14)$$

Employing this exponential equation, water inrush recession from January 13 to March 23, 2015, was calculated and then compared with that observed (Table 3 and Fig. 19). It can be noted that, since February 7, 2015, the decreasing trend of groundwater inrush into the tunnel was slowed down, reaching a constant value, so that after 45 days, the inrush rate into the tunnel has decreased by only about 0.02 m^3/s. This may be due to a change in the flow system from the conduit to the diffuse, or it could arise from the tunnel being at equilibrium with the groundwater system. Such circumstance points out to validity of this method only in the case when the rate of decreasing inrush in tunnels is an exponential function of time (conduit dominant flow); when the rate of decreasing inrush is near-constant, the method is no longer valid.

Table 5 Data statistics in the case studies

	Nosud tunnel		Headrace tunnel		Glas tunnel	
	Q_{ob} (m^3/s)	Q_{cal} (m^3/s)	Q_{ob} (m^3/s)	Q_{cal} (m^3/s)	Q_{ob} (m^3/s)	Q_{cal} (m^3/s)
Number of data	58	58	66	71	11	11
Minimum	1.02	0.75	0.22	0.11	0.19	0.15
Maximum	2.43	2.51	0.29	0.31	0.19	0.19
Mean	1.5013	1.461	0.243	0.195	0.189	0.172
Std. Deviation	0.42276	0.51443	0.02058	0.05718	0.00151	0.01339
Variance	0.179	0.265	0.000	0.003	0.000	0.000

Table 6 Observed (Q_{ob}) and calculated (Q_{cal}) groundwater inrush rates, with the calculation error

Case study	Model description	Regression analysis		Strength	Error analysis				
		R	*R* square		MAE	MSE	RMSE	ME	Percent Decline
Nosud	$Q_{ob}=0.810\times Q_{cal}+1.568$	0.985	0.971	Very highly correlated	0.104	0.016	0.127	0.040	8%
Headrace	$Q_{ob}=0.339*Q_{cal}+0.178$	0.941	0.886	Highly correlated	0.051	0.007	0.083	0.048	22%
Glas	$Q_{ob}=0.339\times Q_{cal}+0.178$	0.867	0.752	Highly correlated	0.017	0.0004	0.020	0.016	9%

Case study 3: The Glas Tunnel

The Glas water conveyance tunnel is a 35.661 km tunnel located in the West Azerbaijan Province, Iran (Fig. 20). The tunnel is under construction to transfer about 650 million m^3 of water annually from the reservoir of Kanisib Dam on Lavin River to the Urmia Lake, with the main purpose of reviving the lake (Golian et al. 2021a). Excavation of this tunnel from two directions (inlet and outlet), with Double Shield and mixed EPB (Earth Pressure Balance)/Open Mode TBMs, with a drilling diameter of 6.42 m and a final diameter of 5.5 m on a slope of 0.008% is currently being carried out. Excavation of the inlet section is from 0 to 15 km, and the outlet is from 15 to 35.661 km.

Geological characteristics of the study area

Based on the geological studies of the tunnel route, the excavation from 0 to 3 km and from 12.6 to 14.8 km will cross alluvial deposits, whilst the remaining will be in rock units. These latter are very diverse and can be divided into three classes of sedimentary (conglomerate and limestone), metamorphic (schist, slate, and marble) and igneous (granite, granodioritic and andesitic intrusions) rocks (Fig. 21).

Event of groundwater inrush to the tunnel

On March 1, 2017, the tunnel encountered a karst conduit (1 m in width, 1.5 m high) in the marble unit at chainage 29.231 km (Fig. 22). The initial volume of water entering the tunnel front was approximately 0.25 m^3/s (Fig. 23). Along with water inrush, a considerable amount of silt and clay sediments entered the tunnel, too, imposing a delay in the tunnel excavation. The water inrush also caused subsidence at the ground surface of agricultural lands in the vicinity (Fig. 24).

Estimation of recession time of the water inrush

When water inrush into the tunnel took place, changes in the inrush rate and GWL drawdown in KST-08 borehole were being monitored on a daily basis (Fig. 25). Using the observed

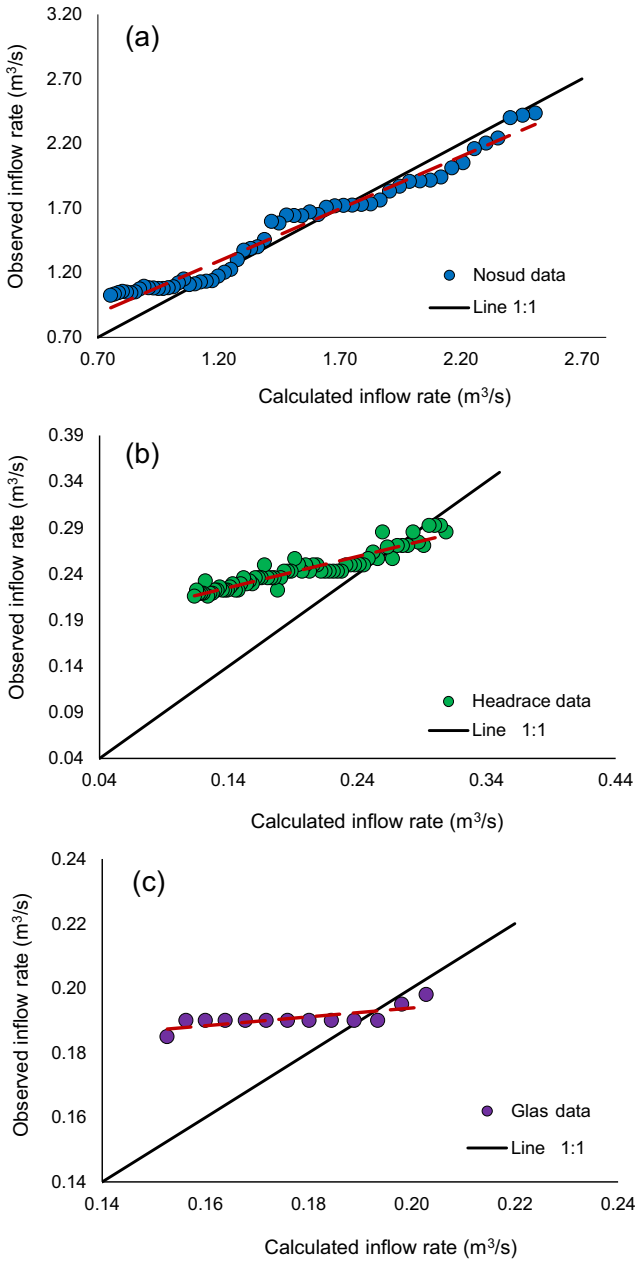

Fig. 29 Correlation curve of the observed and calculated groundwater inrush rates to the front of **a** the Nosud tunnel, **b** the Headrace tunnel, and **c** the Glas tunnel faces

Table 7 Tunnel water inrush calculation error comparison for the proposed method and simple exponential, linear, power, and logarithmic regression models

The Nosud Tunnel				
	Equation	RMSE	Percent decline	R^2
The presented method	$Q_{cal} = 4.34\ e^{-0.021\ t}$	0.127	8%	0.97
Simple exponential	$Q_{cal} = 4.34\ e^{-0.023\ t}$	0.204	14%	0.97
Linear	$Q_{cal} = -0.0719\ t + 4.2297$	1.438	100%	0.92
Power	$Q_{cal} = 4.86\ t^{-0.173}$	0.966	74%	0.97
Logarithmic	$Q_{cal} = -0.569\ \ln(t) + 0.462$	0.899	66%	0.96
The Headrace Tunnel				
	Equation	RMSE	Percent decline	R^2
The presented method	$Q_{cal} = 0.36\ e^{-0.0145\ t}$	0.083	22%	0.88
Simple exponential	$Q_{cal} = 0.35\ e^{-0.0190\ t}$	0.104	37%	0.89
Linear	$Q_{cal} = -0.0061\ t + 0.3528$	0.202	76%	0.84
Power	$Q_{cal} = 0.38\ t^{-0.09}$	0.071	11%	0.96
Logarithmic	$Q_{cal} = -0.03\ \ln(t) + 0.374$	0.068	8%	0.97
The Glas Tunnel				
	Equation	RMSE	Percent decline	R^2
The presented method	$Q_{cal} = 0.25\ e^{-0.0237\ t}$	0.022	9%	0.74
Simple exponential	$Q_{cal} = 0.25\ e^{-0.0281\ t}$	0.033	16%	0.75
Linear	$Q_{cal} = -0.0061\ t + 0.2546$	0.038	17%	0.71
Power	$Q_{cal} = 0.26\ t^{-0.106}$	0.005	2%	0.81
Logarithmic	$Q_{cal} = -0.023\ \ln(t) + 0.257$	0.005	1%	0.82

data from March 1 to 10, 2017 (10 days), according to the presented approach, the related calculations are shown in Eqs. 15 to 17, and the outcomes in Figs. 26 and 27.

$$\ln(H) = -0.006\ t + 4.5252 \tag{15}$$

$$\ln(Q) = 3.942\ \ln(H) - 19.22 \tag{16}$$

$$\ln(Q) = 3.942\ (-0.006\ t + 4.5252) - 19.22 \rightarrow \ln(Q) = -0.0237\ t - 1.38 \rightarrow Q = 0.251\ e^{-0.0237\ t} \tag{17}$$

As presented in Fig. 28 and Table 4, 12 days after the water inrush event, the inrush into the tunnel reached a constant value of 0.19 m^3/s.

Discussion and results

The statistics data of the observed (Q_{ob}) and calculated (Q_{cal}) groundwater inrushes into tunnels are summarized in Table 5.

To validate the estimated groundwater inrushes by the proposed method, first, the correlation of the observed and calculated values was determined using regression analysis (Golian et al. 2019; Fig. 29 and Table 6). As can be seen, there is a very high correlation in the Nosud tunnel and a high correlation in the Headrace and Glas tunnels between Q_{ob} and Q_{cal} data (Shayib 2013). Besides, line 1:1 (the identity line) is used as a reference in the correlation plot to compare two datasets under ideal conditions. When the corresponding data points from the two datasets are equal to each other, the corresponding scatters fall exactly on the identity line. As shown in Fig. 29, according to the identity line, the best dataset is for the Nosud Tunnel, where the flow was dominantly conduit.

The application of regressions techniques for model evaluation has been questioned by some authors (Mitchell 1997; Kobayashi and Salam 2000). It has been suggested that the evaluation of the model alone using the regression model may not be accurate and appropriate so that utilization of the error analysis is strongly recommended (van Tongeren 1995; Knightes and Cyterski 2005). In this study, the error analysis was investigated by different methods such as ME, MSE, MAE, RMSE, and the Percent Decline (or the Percentage Change), the results of which are listed in Table 6. Results of the error analysis indicate that there is a good relationship between Q_{ob} and Q_{cal} data.

The important point to consider in this study is that for the determination of discharge duration in tunnels, the simple exponential regression equation can also be used. In this case, one should fit the measured groundwater inrush against the time to direct and determine its correspondence regression equation. However, it should be noted that due to the very high turbulence of the water inrush, the water inrush measurement may include high errors. For this reason, the exponential equation obtained from the inrush-time regression provides estimations with lower accuracy compared to the method presented in this study (Table 7 and Fig. 29). In the presented

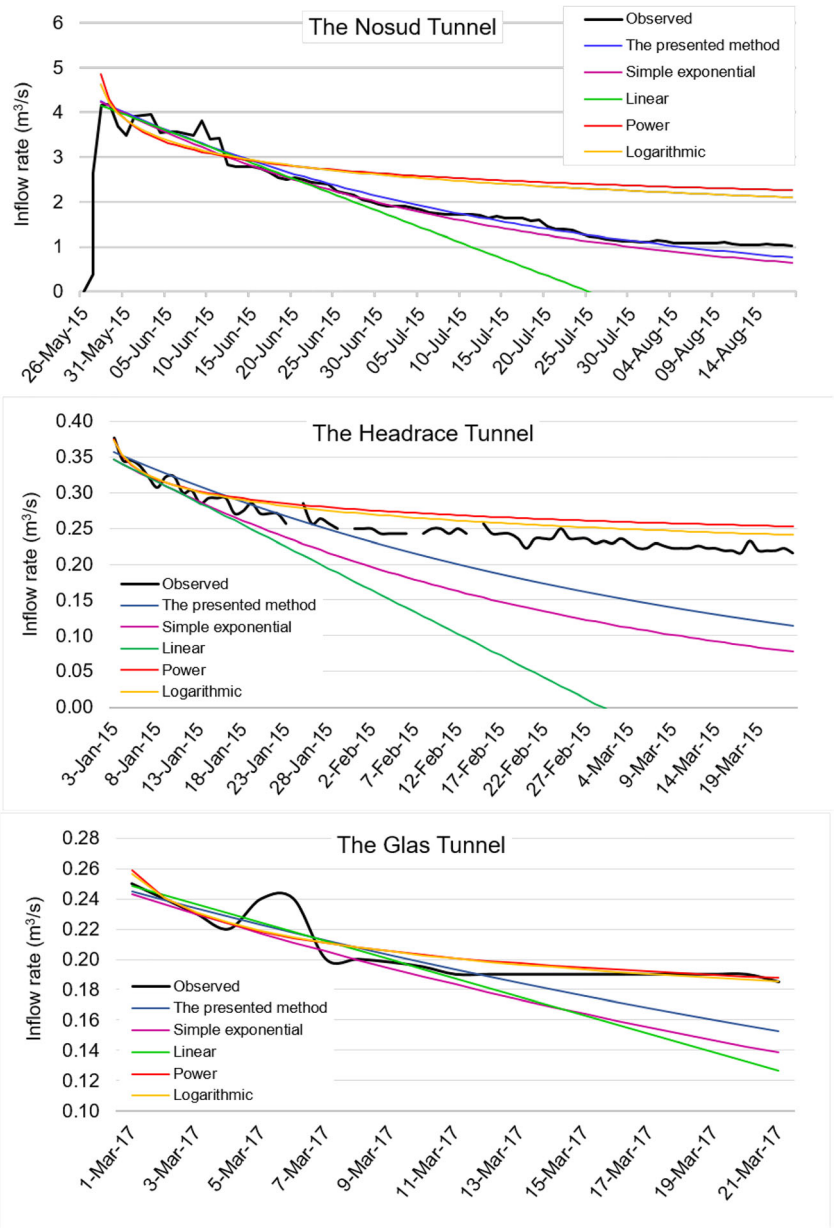

Fig. 30 Comparison of observations with tunnel water inrush calculated with the proposed method and simple exponential, linear, power, and logarithmic regression models

method, to increase the accuracy of the results, the effect of the groundwater level, which is measured with very high accuracy, is also considered. The discharge duration in the tunnels is also calculated by power, logarithmic, and linear regressions and the results are presented in Fig. 30. Linear regression has not been effective in any of the case studies and represents a significant computational error. However, power and logarithmic regressions represent the best fit with the observation curves of Glas and Headrace tunnels with the lowest error, despite the Nosud tunnel with significant errors. In conclusion, considering that the proposed method exhibited acceptable results in all three case studies, the application of this method is recommended instead of the regression models.

Conclusions

The event of water inrush to tunnels in karst terrains and some cases of tunneling in fault zones is a subtle hazard, especially due to inappropriate site investigation, deriving from a combination of human activities (engineering works, in this case, the tunnel excavation) and the natural asset. This latter is extremely difficult to be assessed in karst environments, where the anisotropy and heterogeneity of the rock mass (Andriani and Parise 2015, 2017), and its hydrogeological characteristics (Stevanović et al. 2007 2010; Zini et al. 2015), make carbonate aquifers one of the most problematic situations to be encountered in engineering works (Milanović 2000).

Water inrush in tunnels may cause severe time delays, and financial and life casualties as well. It is of crucial importance to engineers and geologists to calculate the downtime of TBM, as a consequence of water inrush (Palma et al. 2012). This lasts until the flow into the tunnel decreases to the level in which excavation is possible again. To determine water inrush recession time in tunnels, an analytical approach, based on observed inrush rate in tunnels and GWL in nearby boreholes, was introduced and applied to three case studies. The good fit between the observed and estimated curves indicates the efficiency of the applied analytical method. In principle, our conclusions should be validated by a larger number of cases than the considered ones; the authors will be grateful to colleagues who, after trying the method, will want to inform them of the results.

Furthermore, the accuracy of using the Parshall Flume equation within hydrodynamic equations of inrush to tunnel shows that the relationship between discharge and hydraulic head for conduit karstic media and fault zones is a simple power relation.

Acknowledgements The authors are grateful to Lar, Farab and Zistab Consulting Engineers Companies, and Iran Water and Power Resources Development Co. for providing the data. Also, the authors would like to express their gratitude to the editor and the reviewers for spending their time on the manuscript and insist that their comments enabled us to improve the quality of the manuscript.

References

Andriani GF, Parise M (2015) On the applicability of geomechanical models for carbonate rock masses interested by karst processes. Environ Earth Sci 74(12):7813–7821. https://doi.org/10.1007/s12665-015-4596-z

Andriani GF, Parise M (2017) Applying rock mass classifications to carbonate rocks for engineering purposes with a new approach using the rock engineering system. J Rock Mech Geotech Eng 9(2):364–369. https://doi.org/10.1016/j.jrmge.2016.12.001

Bakalowicz M (2005) Karst groundwater: a challenge for new resources. Hydrogeol J 13(1):148–160. https://doi.org/10.1007/s10040-004-0402-9

Bonetto S, Fiorucci A, Fornaro M, Vigna B (2008) Subsidence hazards connected to quarrying activities in a karst area: the case of the Moncalvo sinkhole event (Piedmont, NW Italy). Estonian J Earth Sci 57(3):125–134. https://doi.org/10.3176/earth.2008.3.01

Boussinesq J (1904) Recherche theoruques sur l' écoulement des nappes d'eau infiltrées dans le sol et sur le débit des sources. J Math Pures Appl Fr 10(5):5–78 363-394

Clay RB, Takacs AP (1997) Anticipating the unexpected Flood, fire overbreak, inrush, collapse. In: Tunneling Under Difficult Conditions and Rock Mass Classification, Proceedings of One Day Seminar and International Conference, Basel, Switzerland.

Day MJ (2004) Karstic problems in the construction of Milwaukee's Deep Tunnels. Environ Geol 45(6):859–863. https://doi.org/10.1007/s00254-003-0945-4

De Waele J, Gutierrez F, Parise M, Plan L (2011) Geomorphology and natural hazards in karst areas: a review. Geomorphology 134(1–2):1–8. https://doi.org/10.1016/j.geomorph.2011.08.001

Degallier R (1966) Interpretation de Courbes exponentielles de tarissement. Memories de AIH Beograd:171–172

Dewandel B, Lachassagne P, Bakalowicz M, Weng P, Al-Malki A (2003) Evaluation of aquifer thickness by analysing recession hydrographs. Application to the Oman ophiolite hard-rock aquifer. J Hydrol 274(1-4):248–269. https://doi.org/10.1016/S0022-1694(02)00418-3

Fanchi JR (2002) Shared Earth Modeling: Methodologies for Integrated Reservoir Simulations. Gulf Prof Publ. https://doi.org/10.1016/B978-075067522-2/50000-8

Fiorillo F (2014) The recession of spring hydrographs, focused on karst aquifers. Water Resour Manag 28(7):1781–1805. https://doi.org/10.1007/s11269-014-0597-z

Ford DC, Williams P (2007) Karst hydrogeology and geomorphology. John Wiley & Sons, Chichester

Giese M, Reimann T, Bailly-Comte V, Maréchal JC, Sauter M, Geyer T (2018) Turbulent and laminar flow in karst conduits under unsteady flow conditions: interpretation of pumping tests by discrete conduit-continuum modeling. Water Resour Res 54(3):1918–1933. https://doi.org/10.1002/2017WR020658

Golian M, Katibeh H, Singh VP, Ostad-Ali-Askari K, Tavasoli Rostami H (2019) Prediction of tunneling impact on flow rates of adjacent extraction water wells. Q J Eng Geol Hydrogeol 53(2):236–251. https://doi.org/10.1144/qjegh2019-055

Golian M, Sharifi Teshnizi E, Tavasoli Rostami H, Katibeh H, Parise M, Mahdad M, Saadat H, Abbasi M, Ebad Ardestani M (2021a) Advantages of employing multilevel monitoring wells for design of tunnels subjected to multi-aquifer alluvial. J Mt Sci 18(1):219–232. https://doi.org/10.1007/s11629-020-6293-y

Golian M, Abolghasemi M, Hosseini A, Abbasi M (2021b) Restoring groundwater levels after tunneling: a numerical simulation approach to tunnel sealing decision making. Hydrogeol J. Advance online publication.

Gutiérrez F, Parise M, De Waele J, Jourde H (2014) A review on natural and human-induced geohazards and impacts in karst. Earth Sci Rev 138:61–88. https://doi.org/10.1016/j.earscirev.2014.08.002

Harmon RS, Wicks CM (2006) Perspectives on Karst Geomorphology, Hydrology, and Geochemistry - A Tribute Volume to Derek C. Ford and William B. White. Geol Soc Am. https://doi.org/10.1130/SPE404

Hou T, Yang X, Xing H, Huang K, Zhou J (2016) Forecasting and prevention of water inrush during the excavation process of diversion tunnel at the Jinping II Hydropower Station, China. Springer Plus 5:700. https://doi.org/10.1186/s40064-016-2336-9

Ismail A (2017) Uma Oya Development Project: Multi-purpose or multi-destructive? Daily Mirror online, [online] Available at: http://www.dailymirror.lk/article/Uma-Oya-Development-Project-Multi-purpose-or-multidestructive%2D%2D121570.html [Accessed 3 January 2017]

Knightes CD, Cyterski M (2005) Evaluating predictive errors of a complex environmental model using a general linear model and least square means. Ecol Model 186(3):366–374. https://doi.org/10.1016/j.ecolmodel.2005.01.034

Kobayashi K, Salam MU (2000) Comparing simulated and measured values using mean squared deviation and its components. Agron J 92(2):345–352. https://doi.org/10.2134/agronj2000.922345x

Li L, Tu W, Shi S, Chen J, Zhang Y (2016) Mechanism of water inrush in tunnel construction in the karst area. Geomatics Nat Hazards Risk 7(sup1):35–46. https://doi.org/10.1080/19475705.2016.1181342

Li XH, Zhang QS, Zhang X, LAN XD, DUAN CH, LIU JG (2018) Detection and treatment of water inflow in karst tunnel: A case study in Daba tunnel. J Mt Sci 15(7):1585–1596. https://doi.org/10.1007/s11629-018-4919-0

Maillet E (1905) Essais d'hydraulique souterraine & fluviale (Hydraulic tests in the subsurface and in rivers). Hermann, Paris

Mangin A (1975) Contribution à l'étude hydodynamique des aquifères karstique. Doctorale thése, Univ. Dijon ; Annales de Speléologie, 30 (1), 21-124.

McCallum J, Simmons C, Mallants D, Batelaan O (2016) Simulating the groundwater flow dynamics of fault zones; MODFLOW Un-Structured Grid: A comparison of methods for representing fault properties and a regional implementation. Techn Rep: The Commonwealth Scientific and Industrial Research Organization. https://doi.org/10.13140/RG.2.2.24875.34085

McCormack T, O'Connella E, Daly Y, Gill LW, Henry T, Perriquetc M (2017) Characterization of karst hydrogeology in Western Ireland using geophysical and hydraulic modeling techniques. J Hydrol: Regional Studies 10:1–17. https://doi.org/10.1016/j.ejrh.2016.12.083

Milanović PT (2000) Geological Engineering in Karst: dams, reservoirs, grouting, groundwater protection, water tapping, tunneling: with 190 figures. Zebra, Belgrade, p 347

Milanović P (2002) The environmental impacts of human activities and engineering constructions in karst regions. Episodes 25(1):13–21. https://doi.org/10.18814/epiiugs/2002/v25i1/002

Milanović S (2016) 3D Spatial modeling of karst channels– The Beljanica karst massif. Karst without Boundaries, edt. Z. Stevanović, N. Krešić, N. Kukurić, CRC Press/Balkema, Taylor & Francis Group, 169-188. https://doi.org/10.1201/b21380-15

Milanović S, Vasić LJ (2016) 3D Conduit modeling of leakage below a dam situated in highly karstified rocks. Karst without Boundaries, edt. Z. Stevanović, N. Krešić, N. Kukurić, CRC Press/Balkema, Taylor & Francis Group, 321-336. https://doi.org/10.1201/b21380-27

Mitchell PL (1997) Misuse of regression for empirical validation of models. Agric Syst 54(3):313–326. https://doi.org/10.1016/S0308-521X(96)00077-7

Palma B, Ruocco A, Lollino P, Parise M (2012) Analysis of the behavior of a carbonate rock mass due to tunneling in a karst setting. In: Han KC, Park C, Kim JD, Jeon S, Song JJ (Eds), The present and future of rock engineering. Proceedings of 7th Asian Rock Mechanics Symposium, Seoul, 772–781.

Parise M (2019) Sinkholes. In: White W.B., Culver D.C. & Pipan T. (Eds.), Encyclopedia of Caves. Academic Press, Elsevier, 3rd edition, 934-942.

Parise M, Closson D, Gutierrez F, Stevanović Z (2015a) Anticipating and managing engineering problems in the complex karst environment. Environ Earth Sci 74(12):7823–7835. https://doi.org/10.1007/s12665-015-4647-5

Parise M, Ravbar N, Živanović V, Mikszewski A, Kresić N, Mádl-Szonyi J, Kukurić N (2015b) Hazards in Karst and Managing Water Resources Quality. Chapter 17 in Z. Stevanović (ed.), Karst Aquifers- Characterization and Engineering. Professional Practice in Earth Sciences, Springer, 601-687. https://doi.org/10.1007/978-3-319-12850-4_17

Parise M, Gabrovsek F, Kaufmann G, Ravbar N (2018) Recent advances in karst research: from theory to fieldwork and applications. In: Parise M, Gabrovsek F, Kaufmann G, Ravbar N (Eds.), Advances in Karst Research: Theory, Fieldwork, and Applications. Geological Society, London, Special Publications, 466, 1–24. https://doi.org/10.1144/SP466.26

Parshall R (1928) The improved venture flume. Colorado Agric Coll Bull 336:87

Perriquet M (2014) Characterization of the Hydrodynamics and Saltwater Wedge Variations in a Coastal Karst Aquifer in Response to Tide and Precipitation Events (Bell Harbour Catchment Co. Clare, Ireland). National University of Ireland, Galway (Doctoral dissertation, Montpellier 2).

Qiang Q, Rong X (2008) State, issues, and relevant recommendations for security risk management of China's underground engineering. Chin J Rock Mech Eng 27(4):649–655 (In Chinese). https://doi.org/10.3321/j.issn:1000-6915.2008.04.001

Rathnayake B (2016) Sri-Lanka flood management and social impacts. Water New Zealand Tech J:44–47

Sadeghi S, Sharifi Teshnizi E, Ghoreishi B (2020) Correlations between various rock mass classification / characterization systems for the Zagros tunnel–W Iran. J Mt Sci 17:1790–1806. https://doi.org/10.1007/s11629-019-5665-7

Sauter M (1992) Quantification and forecasting of regional groundwater flow and transport in a karst aquifer (Gallusquelle, Malm, SW Germany). Tubinger Geowissenschaftliche Arbeiten, Part C 13:151

Shayib MA (2013) Applied Statistics. 1st edition, 300 p. ISBN: 978-87-403-0493-0

Shi S, Bu L, Li S, Xiong Z, Xie X, Li L, Zhou Z, Xu Z, Ma D (2017) Application of comprehensive prediction method of water inrush hazards induced by unfavorable geological body in high risk karst tunnel: a case study. Geomatics, Nat Hazards Risk 8(2):1407–1423. https://doi.org/10.1080/19475705.2017.1337656

Stevanović Z (2015) Engineering regulation of karstic spring flow to improve water sources in critical dry periods. In: Stevanović Z (Ed) Karst aquifers– characterization and engineering. Series: Professional Practice in Earth Science. Springer Intern. Publ. Switzerland, 490–530.

Stevanović Z, Jemcov I, Milanović S (2007) Management of karst aquifers in Serbia for water supply. Environ Geol 51(5):743–748. https://doi.org/10.1007/s00254-006-0393-z

Stevanović Z, Milanović S, Ristić V (2010) Supportive methods for assessing effective porosity and regulating karst aquifers. Acta Carsol 39(2):313–329. https://doi.org/10.3986/ac.v39i2.102

Taneeb (2005) Hsuehshan Tunnel. Taiwan Area National Expressway Engineering Bureau, Taiwan

van Tongeren OF (1995) Data analysis or simulation model: a critical evaluation of some methods. Ecol Model 78(1-2):51–60. https://doi.org/10.1016/0304-3800(94)00117-Z

Vigna B, Fioraso G, Banzato C, De Waele J (2010a) Evolution of karst in Messinian gypsum (Monferrato, Northern Italy). Geodin Acta 23(1–3):29–40. https://doi.org/10.3166/ga.23.29-40

Vigna B, Fiorucci A, Banzato C, Forti P, De Waele J (2010b) Hypogene gypsum karst and sinkhole formation at Moncalvo (Asti, Italy). Z Geomorphol, Supplementary Issues 54(2):285–306. https://doi.org/10.1127/0372-8854/2010/0054S2-0015

Waltham AC, Smart PL (1988) Civil engineering difficulties in the karst of China. Q J Eng Geol Hydrogeol 21(1):2–6. https://doi.org/10.1144/gsl.qjeg.1988.021.01.01

Wang G, You G, Xu Y (2008) Investigation on the Nanjing Gypsum Mine Flooding. In: Liu H, Deng A, Chu J (eds) Geotechnical Engineering for Disaster Mitigation and Rehabilitation. Springer-Verlag, Berlin, pp 920–930. https://doi.org/10.1007/978-3-540-79846-0_121

Wang Y, Yin X, Geng F, Jing H, Su H, Liu R (2017) Risk assessment of water inrush in karst tunnels based on the efficacy coefficient method. Pol J Environ Stud 26(4):1765–1775. https://doi.org/10.15244/pjoes/65839

White WB (2002) Karst hydrology: recent developments and open questions. Eng Geol 65(2-3):85–105, Elsevier Science. https://doi.org/10.1016/S0013-7952(01)00116-8

Xu J, Huang S (1996) Mechanism of burst mud and spring water of the Dayaoshan tunnel. J Railway Eng Soc 2:83–89 (In Chinese)

Zhang N, Zheng Q, Elbaz K, Xu Y-S (2020) Water inrush hazards in the Chaoyang Tunnel, Guizhou, China: a preliminary investigation. Water 12(4):1083. https://doi.org/10.3390/w12041083

Zhao Y, Li P, Tian S (2013) Prevention and treatment technologies of railway tunnel water inrush and mud gushing in China. J Rock Mech Geotech Eng 5(6):468–477. https://doi.org/10.1016/j.jrmge.2013.07.009

Zini L, Calligaris C, Cucchi F (2015) The challenge of tunneling through Mediterranean karst aquifers: The case study of Trieste (Italy). Environ Earth Sci 74(1):281–295. https://doi.org/10.1007/s12665-015-4165-5